Advances in Nano Research, *Vol. 9, No. 1 (2020) 33-45*
DOI: https://doi.org/10.12989/anr.2020.9.1.033

On post-buckling characteristics of functionally graded smart magneto-electro-elastic nanoscale shells

Reza Asrari [1], Farzad Ebrahimi*[2] and Mohammad Mahdi Kheirikhah [1]

[1] *Faculty of Industrial and Mechanical Engineering, Qazvin Branch, Islamic Azad University, Qazvin, Iran*
[2] *Department of Mechanical Engineering, Faculty of Engineering, Imam Khomeini International University, Qazvin, Iran*

(*Received December 11, 2018, Revised April 2, 2020, Accepted June 26, 2020*)

Abstract. Geometrically nonlinear buckling of functionally graded magneto-electro-elastic (FG-MEE) nanoshells with the use of classical shell theory and nonlocal strain gradient theory (NSGT) has been analyzed in present research. Mathematical formulation based on NSGT gives two scale coefficients for simultaneous description of structural stiffness reduction and increment. Functional gradation of material properties is described based on power-law formulation. The nanoshell is under a multi-physical field related to applied voltage, magnetic potential, and mechanical load. Exerting a strong electric voltage, magnetic potential or mechanical load may lead to buckling of nanoshell. Taking into account geometric nonlinearity effects after buckling, the behavior of nanoshell in post-buckling regime can be analyzed. Nonlinear governing equations are reduced to ordinary equations utilizing Galerkin's approach and post-buckling curves are obtained based on an analytical procedure. It will be shown that post-buckling curves are dependent on nonlocal/strain gradient parameters, electric voltage magnitude and sign, magnetic potential magnitude and sign and material gradation exponent.

Keywords: post-buckling; classical shell theory; functionally graded material; magneto-electro-elastic material; nonlocal strain gradient theory

1. Introduction

Presenting supreme mechanical performance under electrical and magnetic fields, magneto-electro-elastic (MEE) materials can be introduced as a sort of smart materials with excellent applications in sensing devices, intelligent systems and structures (Pan 2001). Subjecting to an external mechanical force, such smart materials are able to represent electro-magnetic field sensing (Ebrahimi and Barati 2018). Also, subjecting to an electro-magnetic field, these materials experience mechanical deformation (Ramirez *et al*. 2006). As an instance, $BaTiO_3$ and $CoFe_2O_4$ may be combined to each other in order to produce composites of MEE material. Based on the percentages of this two materials, it is possible to describe material properties of the composite such as elastic moduli and piezo-magnetic constants. However, the particles of these materials are not directly combined and it is possible to provide a graded distribution of materials. Actually, functionally graded (FG) materials can be produced with the gradation the two materials (Ebrahimi and Barati 2016, Park *et al*. 2016). Mathematical description of FG materials can be done using a power-law function. In fact, a FG-MEE material may be created and described with specific properties which are varying from $BaTiO_3$ to $CoFe_2O_4$ or contrariwise (Barati and Zenkour 2018).

Mathematical description of nano-sized structural components such as shells can be performed by utilizing several new elasticity theories which differ from classical elasticity theory. Some of these theories are known as nonlocal theory and strain gradient theory which have small-scale parameters in order to explain size-dependent behavior of nano-sized structures (Eltaher *et al*. 2016, Barretta *et al*. 2016, Heydarpour and Malekzadeh 2019). Based on previous researches, a structural stiffness increment has been provided by strain gradient influence. Also, a structural stiffness reduction has been reported based on nonlocal elasticity theory of Eringen (1983). This stiffness reduction is observed for nanoshells leading to lower vibration frequencies and buckling loads compared to macro-size shells (Zeighampour *et al*. 2018). Taking into account the effect of nonlocal elasticity, static/dynamic properties of nano-sized magneto-electro-elastic structures have been investigated by various authors (Ke and Wang 2014, Farajpour *et al*. 2016, Ke *et al*. 2014, Waksmanski and Pan 2017).

Simultaneous effects of nonlocal and strain gradient theory can be captured via a unified theory named nonlocal strain gradient theory (NSGT). As proved by molecular dynamic simulations, the two parameters play an important role in mechanical behaviors of nanostructures (Mehralian *et al*. 2017). In recent years, many authors tried to examine static and dynamical responses of nano-structural components in the framework of NSGT. For example, investigating the propagation of elastic waves in a FG nanoplate in thermal environments has been done by Ebrahimi *et al*. (2016) based on NSGT and a higher order

*Corresponding author, Professor,
E-mail: febrahimy@eng.ikiu.ac.ir

ISSN: 2287-237X (Print), 2287-2388 (Online)

plate theory. NSGT modeling and buckling analysis of a nanobeam based on classic beam theory is carried out by Li and Hu (2015). Utilizing a shear deformation beam theory and NSGT, Lu *et al*. (2017) researched vibrational frequencies of a beam with nano-dimension. Based on NSGT formulation, examination of nonlinear bending/ vibration characteristics of FG nanobeams have been accomplished by Li and Hu (2016). Investigating the propagation of elastic waves in FG magneto-electro-elastic nano-sized plates utilizing NSGT has been carried out by Ebrahimi and Dabbagh (2017). In another study, closed-forms of bending solution and vibration solution for NAGT-modeled FG nanobeams have been introduces by Şimşek (2019). Moreover, wave propagation characteristics of nanoshells possessing magneto-electro-elastic material of functionally graded type are researched by Ma *et al*. (2018). In another work, She *et al*. (2018) researched geometrically nonlinear deflections and frequency curves of a cylindrical nanoshell possessing FG properties in the context of NSGT. In the context of NSGT, Arefi *et al*. (2019) examined bending properties of nano-sized plate structures with bottom and top layers of magneto-electro-elastic material. By searching in the literature, it can be deduced that post-buckling behavior of FG-METE cylindrical nanoshell in the context of NSGT and taking into account geometric nonlinear effects is not explored yet.

Post-buckling analysis of a geometrically nonlinear FG-MEE nanoshell has been performed in the present article taking into account nonlocal and strain gradient effects. Mathematical formulation based on NSGT gives two scale coefficients for simultaneous description of structural stiffness reduction and increment. Functional gradation of material properties is described based on power-law formulation. The nanoshell is exposed to multi-physical fields related to applied voltage, magnetic potential, and mechanical load. The governing equations are presented in the framework of Galerkin's method and then post-buckling curves are analytically derived. The dependency of post-buckling curves to nonlocal/strain gradient parameters, electric voltage magnitude and sign, magnetic potential magnitude and sign and material gradation exponent will be explored and discussed.

2. Nonlocal strain gradient shell modeling

Two scale parameters are embedded in NSGT which are nonlocal parameter (ea) and strain gradient parameter (l). So, stress-strain relationship for NSGT dependents on this two parameters. By knowing that ∇^2 is Laplacian operator, the stress-strain relationship based on NSGT may be written by Lim *et al*. (2015)

$$[1-(ea)^2\nabla^2]\sigma_{ij} = C_{ijkl}[1-l^2\nabla^2]\varepsilon_{kl} \tag{1}$$

Here, C_{ijkl} defines the material properties; σ_{ij} and ε_{kl} are the stress and strain components. By assuming $l = 0$, the stress-strain relation based on nonlocal elasticity theory of Eringen will be achieved.

$$[1-(ea)^2\nabla^2]\sigma_{ij} = C_{ijkl}\varepsilon_{kl} \tag{2}$$

3. Shells made of FG-MEE materials

Power-law function is known as an effectual model for characterizing a functionally graded material. This function is able to describe material distribution in transverse direction. So, it is possible to express each material property (P_f) such as piezo-magnetic and elastic properties in such a way that they vary from top surface (P_t) to bottom surface (P_b) based on following relation (Faleh *et al*. 2018)

$$P_f(z) = (P_t - P_b)(\frac{z}{h}+\frac{1}{2})^p + P_b \tag{3}$$

Material gradient index (p) is able to characterize material distribution in thickness direction of the nanoshell. Here, h is nanoshell thickness.

Up to now there are many theories related to plate/shell structures. In order to develop nonlinear formulation for post-buckling of the nanoshell, well-known classical shell theory has been used in the present paper. Thus, the displacements of nanoshell (u_1, u_2, u_3) may be written based on axial (u), circumferential (v) and transverse (w) field variables as

$$u_1(x,y,z) = u(x,y) - z\frac{\partial w}{\partial x}(x,y) \tag{4}$$

$$u_2(x,y,z) = v(x,y) - \frac{z}{R}\frac{\partial w}{\partial y}(x,y) \tag{5}$$

$$u_3(x,y,z) = w(x,y) \tag{6}$$

The strain field for nanoshells taking into account the nonlinear terms is

$$\begin{aligned}
\varepsilon_{xx} &= \frac{\partial u}{\partial x} - z\frac{\partial^2 w}{\partial x^2} + \frac{1}{2}\left(\frac{\partial w}{\partial x}\right)^2 \\
\varepsilon_{yy} &= \frac{\partial v}{\partial y} - \frac{w}{R} - z\frac{\partial^2 w}{\partial y^2} + \frac{1}{2}\left(\frac{\partial w}{\partial y}\right)^2 \\
\gamma_{xy} &= \frac{\partial u}{\partial y} + \frac{\partial v}{\partial x} - 2z\frac{\partial^2 w}{\partial x \partial y} + \frac{\partial w}{\partial x}\frac{\partial w}{\partial y}
\end{aligned} \tag{7}$$

Considering the fact that MEE nanoshell is under electro-magnetic field with electrical potential (Φ) and magnetic potential (Υ), one can define the potentials in following forms as functions of electrical voltage (V) and magnetic potential intensity (Ω)

$$\Phi(x,y,z) = -cos(\xi z)\phi(x,y) + \frac{2z}{h}V \tag{8}$$

$$\Upsilon(x,y,z) = -cos(\xi z)\gamma(x,y) + \frac{2z}{h}\Omega \tag{9}$$

with $\xi = \pi/h$. Calculating the three-dimensional gradient of electro-magnetic potentials gives the electrical field components (E_x, E_θ, E_z) and magnet field components (H_x, H_θ, H_z) as follows

$$E_x = -\Phi_{,x} = cos(\xi z)\frac{\partial \phi}{\partial x}, \tag{10}$$

$$E_y = -\Phi_{,y} = cos(\xi z)\frac{\partial \phi}{\partial y}, \tag{11}$$

$$E_z = -\Phi_{,z} = -\xi\, sin(\xi z)\phi - \frac{2V}{h} \tag{12}$$

$$H_x = -\Upsilon_{,x} = cos(\xi z)\frac{\partial \gamma}{\partial x}, \tag{13}$$

$$H_y = -\Upsilon_{,y} = cos(\xi z)\frac{\partial \gamma}{\partial y}, \tag{14}$$

$$H_z = -\Upsilon_{,z} = -\xi\, sin(\xi z)\gamma - \frac{2\Omega}{h} \tag{15}$$

All ingredients of stress field, electrical field displacement (D_x, D_y, D_z) and magnetic induction (B_x, B_y, B_z) for a size-dependent shell relevant to NSGT may be written as

$$\begin{aligned}&(1-(ea)^2\nabla^2)\sigma_{xx}\\&=(1-l^2\nabla^2)\left[\tilde{C}_{11}\varepsilon_{xx}+\tilde{C}_{12}\varepsilon_{yy}\right]\\&\quad-\tilde{e}_{31}E_z-\tilde{q}_{31}H_z-\tilde{c}_{11}\tilde{\alpha}_1\Delta T\end{aligned} \tag{16}$$

$$\begin{aligned}&(1-(ea)^2\nabla^2)\sigma_{yy}\\&=(1-l^2\nabla^2)\left[\tilde{C}_{12}\varepsilon_{xx}+\tilde{C}_{11}\varepsilon_{yy}\right]\\&\quad-\tilde{e}_{31}E_z-\tilde{q}_{31}H_z-\tilde{c}_{11}\tilde{\alpha}_1\Delta T\end{aligned} \tag{17}$$

$$(1-(ea)^2\nabla^2)\sigma_{x\theta} = (1-l^2\nabla^2)\tilde{C}_{66}\gamma_{x\theta} \tag{18}$$

$$(1-(ea)^2\nabla^2)D_x = +\tilde{s}_{11}E_x + \tilde{d}_{11}H_x \tag{19}$$

$$(1-(ea)^2\nabla^2)D_y = +\tilde{s}_{11}E_\theta + \tilde{d}_{11}H_\theta \tag{20}$$

$$\begin{aligned}&(1-(ea)^2\nabla^2)D_z\\&=(1-l^2\nabla^2)[\tilde{e}_{31}\varepsilon_{xx}+\tilde{e}_{31}\varepsilon_{yy}]+\tilde{s}_{33}E_z+\tilde{d}_{33}H_z\end{aligned} \tag{21}$$

$$(1-(ea)^2\nabla^2)B_x = +\tilde{d}_{11}E_x + \tilde{\chi}_{11}H_x \tag{22}$$

$$(1-(ea)^2\nabla^2)B_y = +\tilde{d}_{11}E_\theta + \tilde{\chi}_{11}H_\theta \tag{23}$$

$$\begin{aligned}&(1-(ea)^2\nabla^2)B_z\\&=(1-l^2\nabla^2)[\tilde{q}_{31}\varepsilon_{xx}+\tilde{q}_{31}\varepsilon_{yy}]+\tilde{d}_{33}E_z+\tilde{\chi}_{33}H_z\end{aligned} \tag{24}$$

Elastic, piezoelectric and magnetic material characteristics have been respectively marked by C_{ij}, e_{ij} and q_{ij}. For considering plane stress conditions, all material properties are expressed in a new form a follows (Ke *et al*. 2014)

$$\begin{aligned}&\tilde{C}_{11} = C_{11} - \frac{C_{13}^2}{C_{33}}, && \tilde{C}_{12} = C_{12} - \frac{C_{13}^2}{C_{33}},\\&\tilde{C}_{66} = C_{66}, && \tilde{e}_{31} = e_{31} - \frac{C_{13}e_{33}}{c_{33}},\\&\tilde{q}_{31} = q_{31} - \frac{C_{13}q_{33}}{C_{33}}, && \tilde{d}_{11} = \tilde{d}_{11},\\&\tilde{d}_{33} = \tilde{d}_{33} + \frac{q_{33}e_{33}}{C_{33}}, && \tilde{s}_{11} = s_{11},\end{aligned} \tag{25}$$

$$\begin{aligned}&\tilde{s}_{33} = s_{33} + \frac{e_{33}^2}{C_{33}}, && \tilde{\chi}_{11} = \chi_{11},\\&\tilde{\chi}_{33} = \chi_{33} + \frac{q_{33}^2}{C_{33}}, && \tilde{\alpha}_1 = \alpha_1 - \frac{c_{13}\alpha_3}{c_{33}}\end{aligned} \tag{25}$$

If U is strain energy of the nanoshell and V is the work done by applied loadings, one can express

Hamilton's rule using the following relation

$$\int_0^t \delta(U-V)dt = 0 \tag{26}$$

where

$$\begin{aligned}\delta U = \int_V (&\sigma_{xx}\delta\varepsilon_{xx} + \sigma_{xx}^{(1)}\delta\nabla\varepsilon_{xx} + \sigma_{yy}\delta\varepsilon_{yy}\\&+\sigma_{yy}^{(1)}\delta\nabla\varepsilon_{yy} + \sigma_{xy}\delta\gamma_{xy} + \sigma_{xy}^{(1)}\delta\nabla\gamma_{xy}\\&-D_x\delta E_x - D_y\delta E_y - D_z\delta E_z\\&-B_x\delta H_x - B_y\delta H_y - B_z\delta H_z)dV\end{aligned} \tag{27}$$

$$\delta V = \int_V \left(N_{x0}\left(\frac{\partial^2 w}{\partial x^2}\right) + N_{y0}\left(\frac{\partial^2 w}{\partial y^2}\right)\right)\delta w dV \tag{28}$$

There are applied loads along axial and circumferential axes which are showed by $N_{x0}$and N_{y0} and

$$N_{x0} = N_{y0} = N^E + N^H + N^M \tag{29}$$

Applied forces along axial and circumferential axes are a summation of mechanical load (N^M), electrical load (N^E), and magnetic load (N^H) for which

$$N^E = -\int_{-\frac{h}{2}}^{\frac{h}{2}} \tilde{e}_{31}\frac{2V}{h}dz, \quad N^H = -\int_{-h/2}^{h/2} \tilde{q}_{31}\frac{2\Omega}{h}dz \tag{30}$$

By utilizing Eq. (26), gathering the variable coefficients of displacements (δu, δv, δw) results in the below governing equations of NSGT shells

$$\frac{\partial N_{xx}}{\partial x} + \frac{\partial N_{xy}}{\partial y} = 0 \tag{31}$$

$$\frac{\partial N_{xy}}{\partial x} + \frac{\partial N_{yy}}{\partial y} = 0 \tag{32}$$

$$\begin{aligned}&\frac{\partial^2 M_{xx}}{\partial x^2} + 2\frac{\partial^2 M_{xy}}{\partial x \partial y} + \frac{\partial^2 M_{yy}}{\partial y^2} + \frac{N_{yy}}{R}\\&+(N_{x0}+N_{xx})\left(\frac{\partial^2 w}{\partial x^2}\right) + \left(N_{y0}+N_{yy}\right)\left(\frac{\partial^2 w}{\partial y^2}\right)\\&+2N_{xy}\frac{\partial^2 w}{\partial x \partial y} = 0\end{aligned} \tag{33}$$

$$\begin{aligned}\int_{-h/2}^{h/2}\Bigg(&cos(\xi z)\frac{\partial D_x}{\partial x} + cos(\xi z)\frac{\partial D_y}{\partial y}\\&+\xi\, sin(\xi z)D_z\Bigg)dz = 0\end{aligned} \tag{34}$$

$$\int_{-h/2}^{h/2}\left(cos(\xi z)\frac{\partial B_x}{\partial x}+cos(\xi z)\frac{\partial B_y}{\partial y}+\xi\, sin(\xi z)B_z\right)dz=0 \tag{35}$$

It must be noted that N_{rs} and M_{rs} ($rs = xx, xy, yy$) define in-plane forces and bending moments

$$\begin{aligned}
N_{xx}&=\int_{-h/2}^{h/2}(\sigma_{xx}^{(0)}-\nabla\sigma_{xx}^{(1)})dz=N_{xx}^{(0)}-\nabla N_{xx}^{(1)}\\
N_{xy}&=\int_{-h/2}^{h/2}(\sigma_{xy}^{(0)}-\nabla\sigma_{xy}^{(1)})dz=N_{xy}^{(0)}-\nabla N_{xy}^{(1)}\\
N_{yy}&=\int_{-h/2}^{h/2}(\sigma_{yy}^{(0)}-\nabla\sigma_{yy}^{(1)})dz=N_{yy}^{(0)}-\nabla N_{yy}^{(1)}\\
M_{xx}&=\int_{-h/2}^{h/2}z(\sigma_{xx}^{(0)}-\nabla\sigma_{xx}^{(1)})dz=M_{x}^{b(0)}-\nabla M_{xx}^{b(1)}\\
M_{y}&=\int_{-h/2}^{h/2}z(\sigma_{yy}^{(0)}-\nabla\sigma_{yy}^{(1)})dz=M_{y}^{b(0)}-\nabla M_{y}^{b(1)}\\
M_{xy}&=\int_{-h/2}^{h/2}z(\sigma_{xy}^{(0)}-\nabla\sigma_{xy}^{(1)})dz=M_{xy}^{b(0)}-\nabla M_{xy}^{b(1)}
\end{aligned} \tag{36}$$

In above relations

$$\begin{aligned}
N_{ij}^{(0)}&=\int_{-h/2}^{h/2}(\sigma_{ij}^{(0)})dz, \qquad N_{ij}^{(1)}=\int_{-h/2}^{h/2}(\sigma_{ij}^{(1)})dz\\
M_{ij}^{(0)}&=\int_{-h/2}^{h/2}z(\sigma_{ij}^{(0)})dz, \quad M_{ij}^{(1)}=\int_{-h/2}^{h/2}z(\sigma_{ij}^{(1)})dz
\end{aligned} \tag{37}$$

In order to define classical and non-classical stresses, two symbols have been respectively employed as $^{(0)}$ and $^{(1)}$. According to Hamilton's principle, it is possible to derive associated boundary conditions for MEE nanoshell based on n_x and n_y as cosines of direction

$$u=0, or N_{xx}n_x+N_{xy}n_y=0 \tag{38}$$

$$v=0, or N_{xy}n_x+N_{yy}n_y=0 \tag{39}$$

$$w=0, \quad or n_x\left(\frac{\partial M_{xx}}{\partial x}+\frac{\partial M_{xy}}{\partial y}-N_{x0}\frac{\partial w}{\partial x}\right)+n_y\left(\frac{\partial M_{yy}}{\partial y}+\frac{\partial M_{xy}}{\partial x}-N_{y0}\frac{\partial w}{\partial y}\right)=0 \tag{40}$$

$$\frac{\partial w}{\partial x}=0, \quad or \quad M_{xx}n_x+M_{xy}n_y=0 \tag{41}$$

$$\frac{\partial w}{\partial y}=0, \quad or \quad M_{xy}n_x+M_{yy}n_y=0 \tag{42}$$

$$\phi=0, \quad or \quad \int_{-h/2}^{h/2}\big(cos(\xi z)D_x n_x+cos(\xi z)D_y n_y\big)dz=0 \tag{43}$$

$$\gamma=0, \quad or \quad \int_{-h/2}^{h/2}\big(cos(\xi z)B_x n_x+cos(\xi z)B_y n_y\big)dz=0 \tag{44}$$

Calculating the integrals presented in Eq. (36) yields the following relations for MEE nanoshells based upon NSGT as

$$\begin{aligned}
&(1-(ea)^2\nabla^2)N_{xx}\\
&=(1-l^2\nabla^2)\left[A_{11}\left(\frac{\partial u}{\partial x}+\frac{1}{2}\left(\frac{\partial w}{\partial x}\right)^2\right)-B_{11}\frac{\partial^2 w}{\partial x^2}\right.\\
&\left.+A_{12}\left(\frac{\partial v}{\partial y}-\frac{w}{R}+\frac{1}{2}\left(\frac{\partial w}{\partial y}\right)^2\right)-B_{12}\left(\frac{\partial^2 w}{\partial y^2}\right)\right]\\
&+A_{31}^{e}\phi+A_{31}^{m}\gamma
\end{aligned} \tag{45}$$

$$\begin{aligned}
&(1-(ea)^2\nabla^2)M_{xx}\\
&=(1-l^2\nabla^2)\left[B_{11}\left(\frac{\partial u}{\partial x}+\frac{1}{2}\left(\frac{\partial w}{\partial x}\right)^2\right)-D_{11}\frac{\partial^2 w}{\partial x^2}\right.\\
&\left.+B_{12}\left(\frac{\partial v}{\partial y}-\frac{w}{R}+\frac{1}{2}\left(\frac{\partial w}{\partial y}\right)^2\right)-D_{12}\frac{\partial^2 w}{\partial y^2}\right]\\
&+E_{31}^{e}\phi+E_{31}^{m}\gamma
\end{aligned} \tag{46}$$

$$\begin{aligned}
&(1-(ea)^2\nabla^2)N_{\theta\theta}\\
&=(1-l^2\nabla^2)\left[A_{12}\left(\frac{\partial u}{\partial x}+\frac{1}{2}\left(\frac{\partial w}{\partial x}\right)^2\right)-B_{12}\frac{\partial^2 w}{\partial x^2}\right.\\
&\left.+A_{11}\left(\frac{\partial v}{\partial y}-\frac{w}{R}+\frac{1}{2}\left(\frac{\partial w}{\partial y}\right)^2\right)-B_{11}\frac{\partial^2 w}{\partial y^2}\right]\\
&+A_{31}^{e}\phi+A_{31}^{m}\gamma
\end{aligned} \tag{47}$$

$$\begin{aligned}
&(1-(ea)^2\nabla^2)M_{\theta\theta}\\
&=(1-l^2\nabla^2)\left[B_{12}\left(\frac{\partial u}{\partial x}+\frac{1}{2}\left(\frac{\partial w}{\partial x}\right)^2\right)-D_{12}\frac{\partial^2 w}{\partial x^2}\right.\\
&\left.+B_{11}\left(\frac{\partial v}{\partial y}-\frac{w}{R}+\frac{1}{2}\left(\frac{\partial w}{\partial y}\right)^2\right)-D_{11}\frac{\partial^2 w}{\partial y^2}\right]\\
&+E_{31}^{e}\phi+E_{31}^{m}\gamma
\end{aligned} \tag{48}$$

$$\begin{aligned}
&(1-(ea)^2\nabla^2)N_{x\theta}\\
&=(1-l^2\nabla^2)\left[A_{66}\left(\frac{\partial u}{\partial y}+\frac{\partial v}{\partial x}+\frac{\partial w}{\partial x}\frac{\partial w}{\partial y}\right)-2B_{66}\frac{\partial^2 w}{\partial x\partial y}\right]
\end{aligned} \tag{49}$$

$$\begin{aligned}
&(1-(ea)^2\nabla^2)M_{x\theta}\\
&=(1-l^2\nabla^2)\left[B_{66}\left(\frac{\partial u}{\partial y}+\frac{\partial v}{\partial x}+\frac{\partial w}{\partial x}\frac{\partial w}{\partial y}\right)-2D_{66}\frac{\partial^2 w}{\partial x\partial y}\right]
\end{aligned} \tag{50}$$

$$\begin{aligned}
&\int_{-\frac{h}{2}}^{\frac{h}{2}}(1-(ea)^2\nabla^2)D_x\, cos(\xi z)dz\\
&=+F_{11}^{e}\frac{\partial\phi}{\partial x}+F_{11}^{m}\frac{\partial\gamma}{\partial x}
\end{aligned} \tag{51}$$

$$\begin{aligned}
&\int_{-\frac{h}{2}}^{\frac{h}{2}}(1-(ea)^2\nabla^2)D_y\, cos(\xi z)dz\\
&=+F_{22}^{e}\frac{\partial\phi}{\partial y}+F_{22}^{m}\frac{\partial\gamma}{\partial y}
\end{aligned} \tag{52}$$

$$\int_{-\frac{h}{2}}^{\frac{h}{2}}(1-(ea)^2\nabla^2)D_z\xi\,sin(\xi z))dz$$
$$= A_{31}^e\left(\frac{\partial u}{\partial x}+\frac{1}{2}\left(\frac{\partial w}{\partial x}\right)^2\right)+A_{31}^e\left(\frac{\partial v}{\partial y}-\frac{w}{R}+\frac{1}{2}\left(\frac{\partial w}{\partial y}\right)^2\right) \quad (53)$$
$$-E_{31}^e\left(\frac{\partial^2 w}{\partial x^2}+\frac{\partial^2 w}{\partial y^2}\right)-F_{33}^e\phi-F_{33}^m\gamma$$

$$\int_{-\frac{h}{2}}^{\frac{h}{2}}(1-(ea)^2\nabla^2)B_x\,cos(\xi z)dz = +F_{11}^m\frac{\partial\phi}{\partial x}+X_{11}^m\frac{\partial\gamma}{\partial x} \quad (54)$$

$$\int_{-\frac{h}{2}}^{\frac{h}{2}}(1-(ea)^2\nabla^2)B_y\,cos(\xi z)dz = +F_{22}^m\frac{\partial\phi}{\partial y}+X_{22}^m\frac{\partial\gamma}{\partial y} \quad (55)$$

$$\int_{-\frac{h}{2}}^{\frac{h}{2}}(1-(ea)^2\nabla^2)B_z\xi\,sin(\xi z)dz$$
$$= A_{31}^m\left(\frac{\partial u}{\partial x}+\frac{1}{2}\left(\frac{\partial w}{\partial x}\right)^2\right)+A_{31}^m\left(\frac{\partial v}{\partial y}-\frac{w}{R}+\frac{1}{2}\left(\frac{\partial w}{\partial y}\right)^2\right) \quad (56)$$
$$-E_{31}^m\left(\frac{\partial^2 w}{\partial x^2}+\frac{\partial^2 w}{\partial y^2}\right)-F_{33}^m\phi-X_{33}^m\gamma$$

in which

$$\{A_{11},B_{11},D_{11}\}=\int_{-h/2}^{h/2}\tilde{C}_{11}\{1,z,z^2\}dz, \quad (57)$$

$$\{A_{12},B_{12},D_{12}\}=\int_{-h/2}^{h/2}\tilde{C}_{12}\{1,z,z^2\}dz, \quad (58)$$

$$\{A_{66},B_{66},D_{66}\}=\int_{-h/2}^{h/2}\tilde{C}_{66}\{1,z,z^2\}dz, \quad (59)$$

$$\{A_{31}^e,E_{31}^e\}=\int_{-h/2}^{h/2}\tilde{e}_{31}\xi\,sin(\xi z)\{1,z\}\,dz \quad (60)$$

$$\{A_{31}^m,E_{31}^m\}=\int_{-h/2}^{h/2}\tilde{q}_{31}\xi\,sin(\xi z)\{1,z\}\,dz \quad (61)$$

$$\{F_{11}^e,F_{22}^e,F_{33}^e\}=\int_{-h/2}^{h/2}\{\tilde{s}_{11}\,cos^2(\xi z),\tilde{s}_{22}\,cos^2(\xi z),\tilde{s}_{33}\xi^2\,sin^2(\xi z)\}\,dz \quad (62)$$

$$\{F_{11}^m,F_{22}^m,F_{33}^m\}=\int_{-\frac{h}{2}}^{\frac{h}{2}}\{\tilde{d}_{11}\,cos^2(\xi z),\tilde{d}_{22}\,cos^2(\xi z),\tilde{d}_{33}\xi^2\,sin^2(\xi z)\}\,dz \quad (63)$$

$$\{X_{11}^m,X_{22}^m,X_{33}^m\}=\int_{-\frac{h}{2}}^{\frac{h}{2}}\{\tilde{\chi}_{11}\,cos^2(\xi z),\tilde{\chi}_{22}\,cos^2(\xi z),\tilde{\chi}_{33}\xi^2\,sin^2(\xi z)\}\,dz \quad (64)$$

The nonlinear governing equations of MEE nanoshells under magneto-electro-mechanical loading taking into account nonlocal and strain gradient influences can be achieved by placing Eqs. (45)-(56) into Eqs. (31)-(35) as

$$(1-l^2\nabla^2)\left[A_{11}\left(\frac{\partial^2 u}{\partial x^2}+\frac{\partial^2 w}{\partial x^2}\frac{\partial w}{\partial x}\right)-B_{11}\frac{\partial^3 w}{\partial x^3}\right.$$
$$+A_{12}\left(\frac{\partial^2 v}{\partial x\partial y}-\frac{1}{R}\frac{\partial w}{\partial x}+\frac{\partial^2 w}{\partial x\partial y}\frac{\partial w}{\partial y}\right)-B_{12}\frac{\partial^3 w}{\partial x\partial y^2}$$
$$+A_{66}\left(\frac{\partial^2 u}{\partial y^2}+\frac{\partial^2 v}{\partial x\partial y}+\frac{\partial^2 w}{\partial x\partial y}\frac{\partial w}{\partial y}+\frac{\partial w}{\partial x}\frac{\partial^2 w}{\partial y^2}\right) \quad (65)$$
$$\left.-2B_{66}\frac{\partial^3 w}{\partial x\partial y^2}\right]+A_{31}^e\frac{\partial\phi}{\partial x}+A_{31}^m\frac{\partial\gamma}{\partial x}=0$$

$$(1-l^2\nabla^2)\left[A_{66}\left(\frac{\partial^2 u}{\partial x\partial y}+\frac{\partial^2 v}{\partial x^2}+\frac{\partial^2 w}{\partial x^2}\frac{\partial w}{\partial y}+\frac{\partial w}{\partial x}\frac{\partial^2 w}{\partial x\partial y}\right)\right.$$
$$-2B_{66}\frac{\partial^3 w}{\partial x^2\partial y}+A_{12}\left(\frac{\partial^2 u}{\partial x\partial y}+\frac{\partial w}{\partial x}\frac{\partial^2 w}{\partial x\partial y}\right)$$
$$-B_{12}\frac{\partial^3 w}{\partial x^2\partial y}+A_{11}\left(\frac{\partial^2 v}{\partial y^2}-\frac{1}{R}\frac{\partial w}{\partial y}+\frac{\partial^2 w}{\partial y^2}\frac{\partial w}{\partial y}\right) \quad (66)$$
$$\left.-B_{11}\frac{\partial^3 w}{\partial y^3}\right]+A_{31}^e\frac{\partial\phi}{\partial y}+A_{31}^m\frac{\partial\gamma}{\partial y}=0$$

$$(1-l^2\nabla^2)\left[B_{11}\left(\frac{\partial^3 u}{\partial x^3}+\frac{\partial^3 w}{\partial x^3}\frac{\partial w}{\partial x}+\frac{\partial^2 w}{\partial x^2}\frac{\partial^2 w}{\partial x^2}\right)\right.$$
$$-D_{11}\frac{\partial^4 w}{\partial x^4}-2D_{12}\frac{\partial^4 w}{\partial x^2\partial y^2}-4D_{66}\frac{\partial^4 w}{\partial x^2\partial y^2}$$
$$-D_{11}\frac{\partial^4 w}{\partial y^4}+B_{12}\left(\frac{\partial^3 v}{\partial x^2\partial y}-\frac{1}{R}\frac{\partial^2 w}{\partial x^2}+\frac{\partial^3 w}{\partial x^2\partial y}\frac{\partial w}{\partial y}\right.$$
$$\left.+\frac{\partial^2 w}{\partial x\partial y}\frac{\partial^2 w}{\partial x\partial y}\right)+2B_{66}\left(\frac{\partial^3 u}{\partial x\partial y^2}+\frac{\partial^3 v}{\partial x^2\partial y}\right.$$
$$\left.+\frac{\partial^2 w}{\partial x^2}\frac{\partial^2 w}{\partial y^2}+\frac{\partial w}{\partial x}\frac{\partial^3 w}{\partial x\partial y^2}+\frac{\partial^3 w}{\partial x^2\partial y}\frac{\partial w}{\partial y}+\frac{\partial^2 w}{\partial x\partial y}\frac{\partial^2 w}{\partial x\partial y}\right)$$
$$+B_{12}\left(\frac{\partial^3 u}{\partial x\partial y^2}+\frac{\partial w}{\partial x}\frac{\partial^3 w}{\partial x\partial y^2}+\frac{\partial^2 w}{\partial x\partial y}\frac{\partial^2 w}{\partial x\partial y}\right)$$
$$+B_{11}\left(\frac{\partial^3 v}{\partial y^3}-\frac{1}{R}\frac{\partial^2 w}{\partial y^2}+\frac{\partial^3 w}{\partial y^3}\frac{\partial w}{\partial y}+\frac{\partial^2 w}{\partial y^2}\frac{\partial^2 w}{\partial y^2}\right)$$
$$+\frac{A_{12}}{R}\left(\frac{\partial u}{\partial x}+\frac{1}{2}\left(\frac{\partial w}{\partial x}\right)^2\right)-\frac{B_{12}}{R}\frac{\partial^2 w}{\partial x^2} \quad (67)$$
$$\left.+\frac{A_{11}}{R}\left(\frac{\partial v}{\partial y}-\frac{w}{R}+\frac{1}{2}\left(\frac{\partial w}{\partial y}\right)^2\right)-\frac{B_{11}}{R}\frac{\partial^2 w}{\partial y^2}\right]$$
$$+E_{31}^e\left(\frac{\partial^2\phi}{\partial x^2}+\frac{\partial^2\phi}{\partial y^2}\right)+E_{31}^m\left(\frac{\partial^2\gamma}{\partial x^2}+\frac{\partial^2\gamma}{\partial y^2}\right)$$
$$+\frac{A_{31}^e}{R}\phi+\frac{A_{31}^m}{R}\gamma$$
$$+(1-(ea)^2\nabla^2)((1-l^2\nabla^2)\left[A_{11}\left(\frac{\partial u}{\partial x}+\frac{1}{2}\left(\frac{\partial w}{\partial x}\right)^2\right)\right.$$
$$\left.-B_{11}\frac{\partial^2 w}{\partial x^2}+A_{12}\left(\frac{\partial v}{\partial y}-\frac{w}{R}+\frac{1}{2}\left(\frac{\partial w}{\partial y}\right)^2\right)-B_{12}\left(\frac{\partial^2 w}{\partial y^2}\right)\right]$$
$$+A_{31}^e\phi+A_{31}^m\gamma)\left(\frac{\partial^2 w}{\partial x^2}\right)2(1-(ea)^2\nabla^2)((1-l^2\nabla^2)$$

$$\left[A_{66}\left(\frac{\partial u}{\partial y}+\frac{\partial v}{\partial x}+\frac{\partial w}{\partial x}\frac{\partial w}{\partial y}\right)-2B_{66}\frac{\partial^2 w}{\partial x\partial y}\right)\left(\frac{\partial^2 w}{\partial x\partial y}\right)$$
$$+(1-(ea)^2\nabla^2)((1-l^2\nabla^2)\left[A_{12}\left(\frac{\partial u}{\partial x}+\frac{1}{2}\left(\frac{\partial w}{\partial x}\right)^2\right)\right.$$
$$\left.-B_{12}\frac{\partial^2 w}{\partial x^2}+A_{11}\left(\frac{\partial v}{\partial y}-\frac{w}{R}+\frac{1}{2}\left(\frac{\partial w}{\partial y}\right)^2\right)-B_{11}\frac{\partial^2 w}{\partial y^2}\right] \quad (67)$$
$$+A_{31}^{e}\phi+A_{31}^{m}\gamma)\left(\frac{\partial^2 w}{\partial y^2}\right)+(1-(ea)^2\nabla^2)$$
$$\left[-(N^E+N^H+N^M)\left(\frac{\partial^2 w}{\partial x^2}+\frac{\partial^2 w}{\partial y^2}\right)\right]=0$$

$$+F_{11}^{e}\frac{\partial^2\phi}{\partial x^2}+F_{11}^{m}\frac{\partial^2\gamma}{\partial x^2}+F_{22}^{e}\frac{\partial^2\phi}{\partial y^2}+F_{22}^{m}\frac{\partial^2\gamma}{\partial y^2}$$
$$+A_{31}^{e}\left(\frac{\partial u}{\partial x}+\frac{1}{2}\left(\frac{\partial w}{\partial x}\right)^2+\frac{\partial v}{\partial y}-\frac{w}{R}+\frac{1}{2}\left(\frac{\partial w}{\partial y}\right)^2\right) \quad (68)$$
$$-E_{31}^{e}\left(\frac{\partial^2 w}{\partial x^2}+\frac{\partial^2 w}{\partial y^2}\right)-F_{33}^{e}\phi-F_{33}^{m}\gamma=0$$

$$+F_{11}^{m}\frac{\partial^2\phi}{\partial x^2}+X_{11}^{m}\frac{\partial^2\gamma}{\partial x^2}+F_{22}^{m}\frac{\partial^2\phi}{\partial y^2}+X_{22}^{m}\frac{\partial^2\gamma}{\partial y^2}$$
$$+A_{31}^{m}\left(\frac{\partial u}{\partial x}+\frac{1}{2}\left(\frac{\partial w}{\partial x}\right)^2+\frac{\partial v}{\partial y}-\frac{w}{R}+\frac{1}{2}\left(\frac{\partial w}{\partial y}\right)^2\right) \quad (69)$$
$$-E_{31}^{m}\left(\frac{\partial^2 w}{\partial x^2}+\frac{\partial^2 w}{\partial y^2}\right)-F_{33}^{m}\phi-X_{33}^{m}\gamma=0$$

4. Solution of nonlinear governing equations

Post-bucking curves of a FG-MEE nanoshell have been obtained thorough solving the nonlinear governing equations based on Galerkin's method and also an analytical procedure. Obtained governing equations from Hamiltons' principle imply that

$$\phi=\gamma=0 \quad (70)$$

on electric and magnetic displacements

$$w=\frac{\partial^2 w}{\partial x^2}=\frac{\partial^4 w}{\partial x^4}=0 \quad (71)$$

on deflection

The displacements should be carefully specified until they satisfy afore-mentioned boundary conditions. Thus, an approximate form of the five displacements may be determined by

$$u=\sum_{m=1}^{\infty}\sum_{n=1}^{\infty}U_{mn}\bar{u}(x,y)=\sum_{m=1}^{\infty}\sum_{n=1}^{\infty}U_{mn}\frac{\partial X_m(x)}{\partial x}Y_n(y) \quad (72)$$

$$v=\sum_{m=1}^{\infty}\sum_{n=1}^{\infty}V_{mn}\bar{v}(x,y)=\sum_{m=1}^{\infty}\sum_{n=1}^{\infty}V_{mn}X_m(x)\frac{\partial Y_n(y)}{\partial y} \quad (73)$$

$$w=\sum_{m=1}^{\infty}\sum_{n=1}^{\infty}W_{mn}\bar{w}(x,y)=\sum_{m=1}^{\infty}\sum_{n=1}^{\infty}W_{mn}X_m(x)\,Y_n(y) \quad (74)$$

$$\phi=\sum_{m=1}^{\infty}\sum_{n=1}^{\infty}\Phi_{mn}\bar{\phi}(x,y)=\sum_{m=1}^{\infty}\sum_{n=1}^{\infty}\Phi_{mn}X_m(x)\,Y_n(y) \quad (75)$$

$$\gamma=\sum_{m=1}^{\infty}\sum_{n=1}^{\infty}\Upsilon_{mn}\bar{\gamma}(x,y)=\sum_{m=1}^{\infty}\sum_{n=1}^{\infty}\Upsilon_{mn}X_m(x)\,Y_n(y) \quad (76)$$

where maximum amplitudes are defined as: U_{mn}, V_{mn}, W_{mn}, Φ_{mn} and Υ_{mn}. Test functions X_m and Y_n should be chosen in proper formation to capture the impacts of boundary condition when two edges are simply-supported (S-S)

$$X_m=sin\left(\frac{m\pi}{L}x\right) \quad (77)$$

$$\boldsymbol{Y_n=Sin(ny)} \quad (78)$$

Considering Galerkin's approach and placing displacement variables presented by Eqs. (72)-(76) into Eqs. (65)-(69) yields the following ordinary nonlinear governing equations as

$$k_{11}U+k_{21}V+k_{31}W+n_1W^2+k_{41}\Phi+k_{51}\Upsilon=0 \quad (79)$$

$$k_{12}U+k_{22}V+k_{32}W+n_2W^2+k_{42}\Phi+k_{52}\Upsilon=0 \quad (80)$$

$$k_{13}U+k_{23}V+k_{33}W+n_3W^2+n_4W^3+n_5UW+n_6VW+k_{43}\Phi+k_{53}\Upsilon+n_9\Phi W+n_{10}\Upsilon W=0 \quad (81)$$

$$k_{14}U+k_{24}V+k_{34}W+n_7W^2+k_{44}\Phi+k_{54}\Upsilon=0 \quad (82)$$

$$k_{15}U+k_{25}V+k_{35}W+n_8W^2+k_{45}\Phi+k_{55}\Upsilon=0 \quad (83)$$

in which n_i and k_{ij} are the components of nonlinear and linear stiffness matrices which can be written in the forms provided in Appendix.

Due to the fact that there are five coupled nonlinear governing equations, presenting a closed-form of buckling load as a function of maximum amplitude (W) is very difficult. Here, with the help of simultaneously solving of Eqs. (84), (85), (87) and (88), it is possible to find amplitudes (U, V, Φ, Υ) as functions of transverse amplitude or maximum deflection (W). However, obtained amplitude have very complicated forms and it is not possible to provide a closed-form for them. So, for simplicity they are defined in new form as

$$U\to\widehat{U}(W) \qquad V\to\widehat{V}(W)$$
$$\Phi\to\widehat{\Phi}(W) \qquad \Upsilon\to\widehat{\Upsilon}(W) \quad (84)$$

Then, obtained amplitude are inserted into Eq. (86) in order to find a single nonlinear governing equation for nanoshell as

$$k_{13}\widehat{U}+k_{23}\widehat{V}+k_{33}W+n_3W^2+n_4W^3+n_5\widehat{U}W+n_6\widehat{V}W+k_{43}\widehat{\Phi}+k_{53}\widehat{\Upsilon}+n_9\widehat{\Phi}W+n_{10}\widehat{\Upsilon}W=0 \quad (85)$$

This equation must solved to obtain buckling loads as a function of W. Also, some normalized parameters can be introduced in this paper such as

$$\bar{N} = N^M \frac{L}{c_{11}^t h}, \quad \mu = \frac{ea}{L}, \quad \lambda = \frac{l}{L}, \quad \widetilde{W} = W\frac{\delta}{h}, \quad \delta = \frac{\pi^2 Rh}{L^2} \tag{86}$$

5. Numerical results and discussions

Geometrically nonlinear buckling of functionally graded magneto-electro-elastic (FG-MEE) nanoshell shown in Fig. 1 has been analyzed in the present section. Mathematical formulation based on NSGT gives two scale coefficients for simultaneous description of structural stiffness reduction and increment. Functional gradation of material properties presented in Table 1 is described based on power-law formulation. The nanoshell is under a multi-physical field related to applied voltage, magnetic field intensity, and mechanical load. First, obtained buckling loads are compared with previous data in literature.

Post-buckling load of a FG cylindrical shell obtained by presented study is compared with that provided by Bitch *et al*. (2013) as shown in Fig. 2. In this figure, a FG shell with material gradient indices p = 1, 5 and the length of L = 2R has been considered. Obtained buckling curves completely matches with that provided by Bich *et al*. (2013). Also, in another comparison study, buckling loads of a nanoshell with 2 nm radius which is modeled by NSGT have been verified in Table 2 with those presented by Mehralian *et al*. (2017). They used molecular dynamic simulation (MDS) to obtain linear buckling loads of a nanoshell based on proper values of nonlocal and strain gradient parameters. Based on the values reported for the two parameters, obtained buckling loads are matched with those provided by Mehralian *et al*. (2017). Also, for validating buckling loads of a FG cylindrical shell, obtained buckling loads are compared with the results provided by Bitch *et al*. (2013) in Table 2 for two buckling modes of (m,n) = (1,3) and (1,5). Different values of material exponent (p = 0, 0.5, 1, 5) are

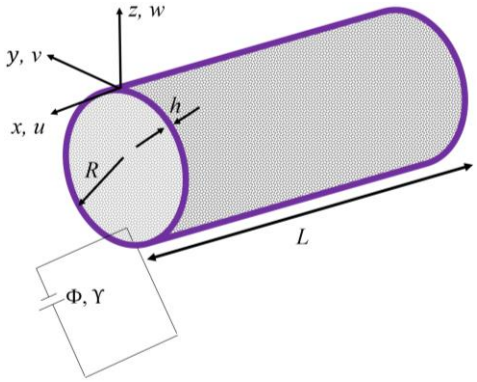

Fig. 1 Configuration of MEE cylindrical nanoshell

Table 1 Material properties of the FG-METE nanoshell

Properties	$BaTiO_3$	$CoFe_2O_4$
$c_{11} = c_{22}$ (GPa)	166	286
c_{12}	77	173
c_{66}	44.5	56.5
e_{31} (Cm^{-2})	-4.4	0
e_{15}	11.6	0
q_{31} (N/Am)	0	580.3
q_{15}	0	550
s_{11} ($10^{-9}C^2m^{-2}N^{-1}$)	11.2	0.08
s_{33}	12.6	0.093
$\chi_{11}(10^{-6}Ns^2C^{-2}/2)$	5	-590
χ_{33}	10	157
$d_{11} = d_{22} = d_{33}$	0	0
$\alpha_1(10^{-6}1/K)$	10	15.7

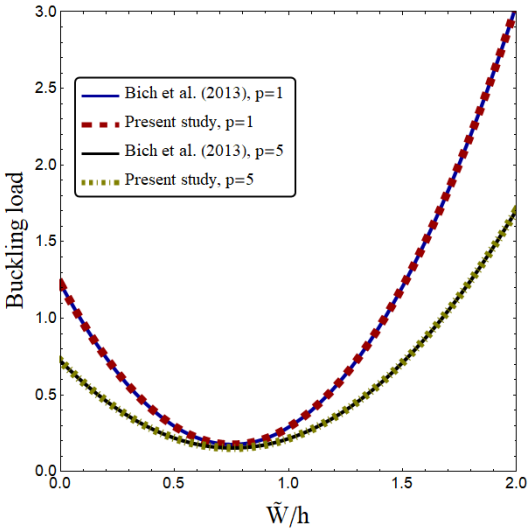

Fig. 2 Verification of post-buckling curves for FG shells

Table 2 Verification of buckling load for NSGT nanoshells (L/R = 10, h/R = 0.2)

	λ = 0.5 nm^2		λ = 0.7 mn^2	
	Mehralian *et al*. (2017)	Present	Mehralian *et al*. (2017)	Present
μ = 1	372.225	372.880	395.186	395.881
μ =1.3	324.044	324.614	344.033	344.638
μ =1.5	293.239	293.775	311.327	311.875

Table 3 Comparison of buckling load for a FG cylindrical shell (R/h = 100)

		Bitch *et al*. (2013)	Present study
L/R = 2	p = 0	2.229	2.229
(m,n) = (1,5)	p = 0.5	1.545	1.545
	p = 1	1.228	1.228
	p = 5	0.723	0.723
L/R = 6	p = 0	2.079	2.079
(m,n) = (1,3)	p = 0.5	1.445	1.445
	p = 1	1.151	1.150
	p = 5	0.674	0.674

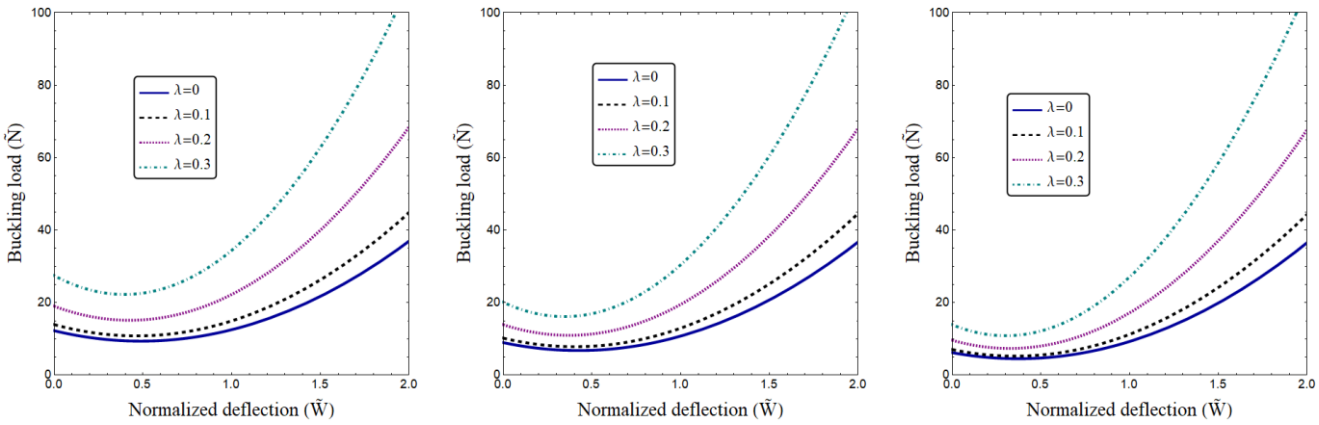

(a) μ = 0.1 (b) μ =0.2 (c) μ = 0.3

Fig. 3 Post-buckling load versus normalized deflection based on various nonlocal and strain gradient parameters (V = 0, Ω = 0, p = 1, L = 2R, R/h = 100)

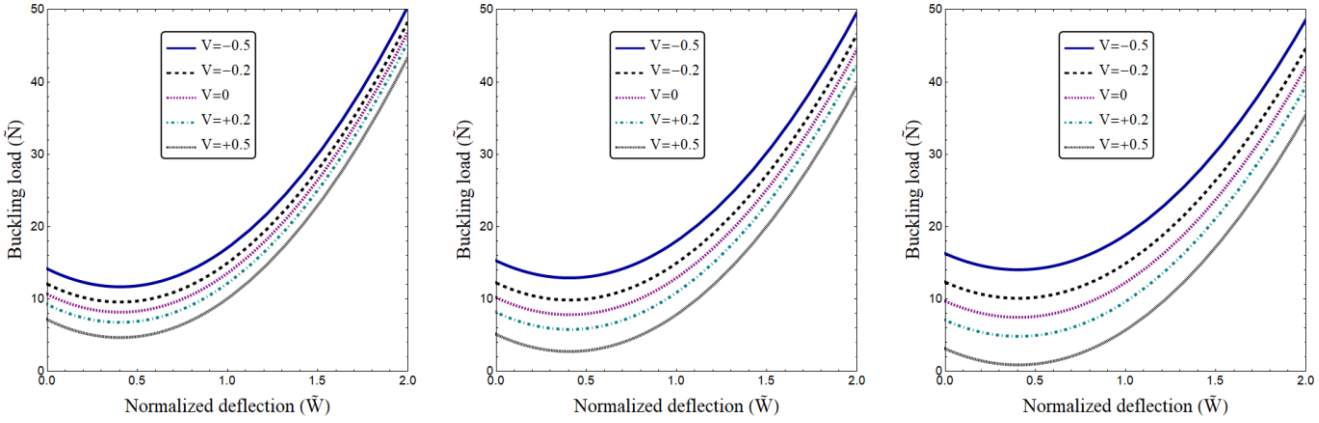

(a) p = 0.5 (b) p = 1 (c) p = 2

Fig. 4 Post-buckling load versus normalized deflection based on various electric voltages and material indices (Ω = 0, μ = 0.2, λ = 0.1, L = 2R, R/h = 100)

considered for this comparison.

Fig. 3 illustrates buckling load of FG-MEE nanoshell versus normalized deflection based on various nonlocal and strain gradient parameters when L = 2R and R/h = 100. For all curves, obtained buckling load at $\tilde{W} = 0$ is called critical buckling load. With increase of normalized deflection, post-buckling curves exhibit an interesting and surprising behavior. In fact, the buckling load of nanoshell first reduces with increase of normalized deflection then it increases. So, immediately after the critical buckling load, the nanoshell has no post-buckling capability and buckling load will reduce. It means that the nanoshell can be subjected to higher deformations under smaller loads. However, the buckling load will increase at higher normalized deflections where the nanoshell can endure higher loads. Another observation from this figure is that post-buckling curves of the nanoshell are influenced by nonlocal and strain gradient effects. Post-buckling curves move higher with increase of strain gradient parameter which introduces structural stiffening effect. Also, post-buckling loads become lower with increase of nonlocal parameter which introduces structural softening effect. In special cases when $\mu = \lambda = 0$, post-buckling curves of a macro size MEE shell can be obtained. Also, assuming only $\lambda = 0$ gives post-buckling curves of nonlocal MEE nanoshells discarding strain gradient effects.

Influences of applied electric voltage (V) and material gradient index (p) on post-buckling curves of a FG-MEE nanoshell have been illustrated in Fig. 4 when μ = 0.2 and λ = 0.1. It can be deduced that post-buckling curves of FG-MEE nanoshells rely on the value of material gradient index. Indeed, increase of material index yields lower post-buckling loads because the amount of $CoFe_2O_4$ having lower elastic moduli is decreased compared to the amount of $BaTiO_3$. Also, as the value of p is smaller, the post-buckling curves based on various values of applied electric voltage become closer to each other. It is due to the fact that at smaller values of p, the portion of $CoFe_2O_4$ in FG material is more than $BaTiO_3$. Since $CoFe_2O_4$ has a zero piezoelectric constant ($e_{31} = 0$) according to Table 1, electric field effects on post-buckling curves reduces at higher portion of $CoFe_2O_4$ or lower values of material index. Also, it may be observed from the figure that negative voltage gives higher post-buckling curves than positive voltage. Actually, positive voltage may induce an axial compressive load to the nanoshell leading to lower structural stiffness

and buckling loads.

Fig. 5 indicates the effects of magnetic field intensity (Ω) and material gradient index (p) on post-buckling curves of a FG-MEE nanoshell modeled by NSGT. As mentioned before, larger values of material gradient index are corresponding to lower buckling loads. Moreover, as the value of p is larger, the post-buckling curves according to various values of magnetic field intensity become closer to

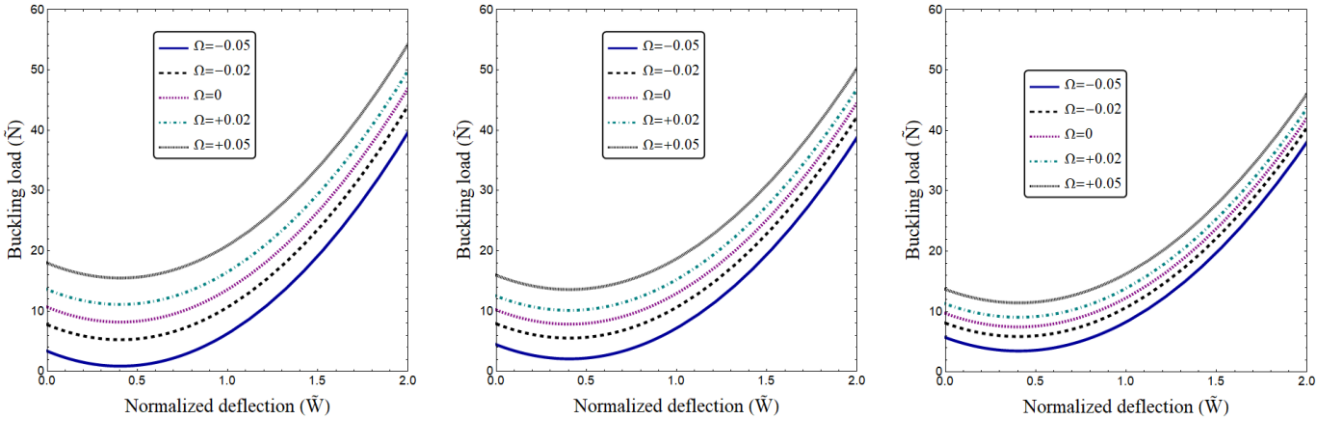

(a) p = 0.5 (b) p = 1 (c) p = 2

Fig. 5 Post-buckling load versus normalized deflection based on various electric magnetic field intensities and material indices (V = 0, μ = 0.2, λ = 0.1, L = 2R, R/h = 100)

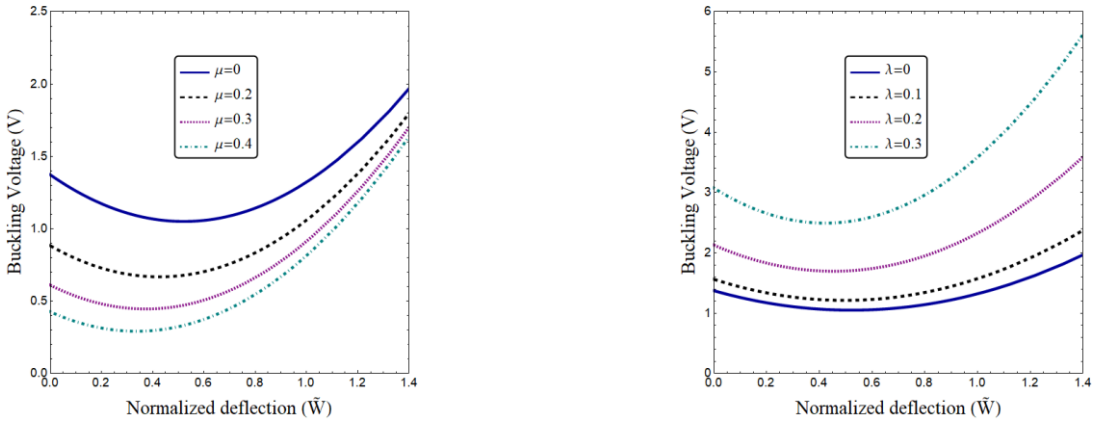

(a) λ = 0 (b) μ = 0

Fig. 6 Buckling voltage versus normalized deflection based on various electric voltages and material indices (Ω = 0, p = 1, L = 2R, R/h = 100)

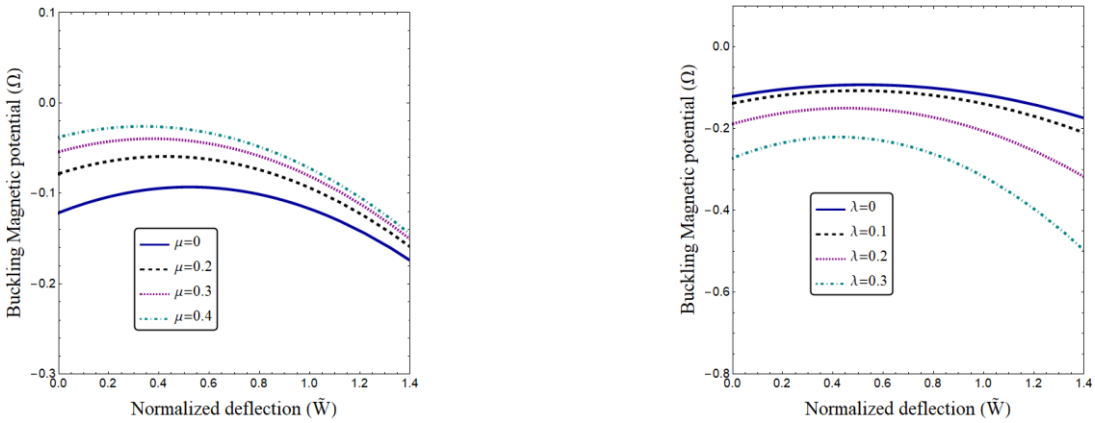

(a) λ = 0 (b) μ = 0

Fig. 7 Buckling magnetic potential versus normalized deflection based on various nonlocal and strain gradient parameters (p = 1, L = 2R, R/h = 100)

each other. The reason is due to the fact that at larger values of p, the portion of $CoFe_2O_4$ in FG material is less than $BaTiO_3$. Since $BaTiO_3$ has a zero magnetic constant (q_{31} = 0) according to Table 1, magnetic field effects on post-buckling curves become less sensible at higher percentages of $BaTiO_3$ or larger values of material index. Furthermore, it may be seen from the figure that negative magnetic field intensity gives lower post-buckling curves than positive magnetic field intensity. Indeed, negative magnetic field intensity leads to lower structural stiffness by exerting an axial compressive load to the nanoshell.

From a scientific point of view, buckling occurs when the structures is subjected to a large compressive load. This load can be a mechanical load acting in axial direction leading to buckling of a nanoshell. Also, the nanoshell may buckle under an intense electric or magnetic field. The voltage in which the nanoshell buckles is called buckling voltage and also the magnetic potential in which the nanoshell buckles is called buckling magnetic potential. Figs. 6 and 7 respectively depict buckling voltage and buckling magnetic potential with respect to normalized maximum deflection and various values of nonlocal and strain gradient parameters. As can be seen, the nanoshell is buckled at negative values of magnetic potential due to the fact that negative magnetic potential can exert a compressive load. In contrast, the nanoshell is also buckled at positive values of electric voltage according to Fig.6. Considering absolute values of buckling voltage and magnetic potential, the post-buckling curves first diminishes with increase of normalized deflection. Then, the post-buckling curves will rise at higher values of normalized deflection. As mentioned before, the cylindrical nanoshells have no post-buckling capability immediately after critical buckling values.

6. Conclusions

An investigation on post-buckling behavior of FG-MEE cylindrical nanoshells under mechanical, electrical and magnetic loadings was presented in the article. Mathematical formulation based on NSGT gave two scale coefficients for simultaneous description of structural stiffness reduction and increment. Functional gradation of material properties was described based on power-law formulation. The governing equations were presented in the framework of Galerkin's method and then post-buckling curves were obtained as functions of maximum deflection. It was seen that the buckling load of nanoshell first reduced with increase of maximum deflection and then it increased. In fact, immediately after the critical buckling load, the nanoshell had no post-buckling capability and buckling load reduced. Another observation from this figure was that post-buckling curves of the nanoshell were influenced by nonlocal and strain gradient effects. It was also seen that increase of material index led to lower post-buckling loads because the amount of $CoFe_2O_4$ having lower elastic moduli was decreased compared to the amount of $BaTiO_3$. Also, as the value of p was smaller, the post-buckling curves based on various values of applied electric voltage became closer to each other.

References

Arefi, M., Kiani, M. and Rabczuk, T. (2019), "Application of nonlocal strain gradient theory to size dependent bending analysis of a sandwich porous nanoplate integrated with piezomagnetic face-sheets", *Compos. Part B: Eng.*, **168**, 320-333. https://doi.org/10.1016/j.compositesb.2019.02.057

Barati, M.R. and Zenkour, A.M. (2018), "Electro-thermoelastic vibration of plates made of porous functionally graded piezoelectric materials under various boundary conditions", *J. Vib. Control*, **24**(10), 1910-1926. https://doi.org/10.1177%2F1077546316672788

Barretta, R., Feo, L., Luciano, R., de Sciarra, F.M. and Penna, R. (2016), "Functionally graded Timoshenko nanobeams: a novel nonlocal gradient formulation", *Compos. Part B: Eng.*, **100**, 208-219. https://doi.org/10.1016/j.compositesb.2016.05.052

Bich, D.H., Nguyen, N.X. and Van Tung, H. (2013), "Postbuckling of functionally graded cylindrical shells based on improved Donnell equations", *Vietnam J. Mech.*, **35**(1), 1-15. https://doi.org/10.15625/0866-7136/35/1/2894

Ebrahimi, F. and Barati, M.R. (2016), "Static stability analysis of smart magneto-electro-elastic heterogeneous nanoplates embedded in an elastic medium based on a four-variable refined plate theory", *Smart Mater. Struct.*, **25**(10), 105014. https://doi.org/10.1088/0964-1726/25/10/105014

Ebrahimi, F. and Barati, M.R. (2018), "Vibration analysis of smart piezoelectrically actuated nanobeams subjected to magneto-electrical field in thermal environment", *J. Vib. Control*, **24**(3), 549-564. https://doi.org/10.1177%2F1077546316646239

Ebrahimi, F. and Dabbagh, A. (2017), "On flexural wave propagation responses of smart FG magneto-electro-elastic nanoplates via nonlocal strain gradient theory", *Compos. Struct.*, **162**, 281-293. https://doi.org/10.1016/j.compstruct.2016.11.058

Ebrahimi, F., Barati, M.R. and Dabbagh, A. (2016), "A nonlocal strain gradient theory for wave propagation analysis in temperature-dependent inhomogeneous nanoplates", *Int. J. Eng. Sci.*, **107**, 169-182. https://doi.org/10.1016/j.ijengsci.2016.07.008

Eltaher, M.A., Khater, M.E. and Emam, S.A. (2016), "A review on nonlocal elastic models for bending, buckling, vibrations, and wave propagation of nanoscale beams", *Appl. Mathe. Model.*, **40**(5-6), 4109-4128. https://doi.org/10.1016/j.apm.2015.11.026

Eringen, A.C. (1983), "On differential equations of nonlocal elasticity and solutions of screw dislocation and surface waves", *J. Appl. Phys.*, **54**(9), 4703-4710. https://doi.org/10.1063/1.332803

Faleh, N.M., Ahmed, R.A. and Fenjan, R.M. (2018), "On vibrations of porous FG nanoshells", *Int. J. Eng. Sci.*, **133**, 1-14. https://doi.org/10.1016/j.ijengsci.2018.08.007

Farajpour, A., Yazdi, M.H., Rastgoo, A., Loghmani, M. and Mohammadi, M. (2016), "Nonlocal nonlinear plate model for large amplitude vibration of magneto-electro-elastic nanoplates", *Compos. Struct.*, **140**, 323-336. https://doi.org/10.1016/j.compstruct.2015.12.039

Heydarpour, Y. and Malekzadeh, P. (2019), "Dynamic stability of cylindrical nanoshells under combined static and periodic axial loads", *J. Brazil. Soc. Mech. Sci. Eng.*, **41**(4), 184. https://doi.org/10.1007/s40430-019-1675-1

Ke, L.L. and Wang, Y.S. (2014), "Free vibration of size-dependent magneto-electro-elastic nanobeams based on the nonlocal theory", *Physica E: Low-dimens. Syst. Nanostruct.*, **63**, 52-61. https://doi.org/10.1016/j.physe.2014.05.002

Ke, L.L., Wang, Y.S., Yang, J. and Kitipornchai, S. (2014), "The size-dependent vibration of embedded magneto-electro-elastic cylindrical nanoshells", *Smart Mater. Struct.*, **23**(12), 125036. https://doi.org/10.1088/0964-1726/23/12/125036

Li, L. and Hu, Y. (2015), "Buckling analysis of size-dependent

nonlinear beams based on a nonlocal strain gradient theory", *Int. J. Eng. Sci.*, **97**, 84-94. https://doi.org/10.1016/j.ijengsci.2015.08.013

Li, L. and Hu, Y. (2016), "Nonlinear bending and free vibration analyses of nonlocal strain gradient beams made of functionally graded material", *Int. J. Eng. Sci.*, **107**, 77-97. https://doi.org/10.1016/j.ijengsci.2016.07.011

Lim, C.W., Zhang, G. and Reddy, J.N. (2015), "A higher-order nonlocal elasticity and strain gradient theory and its applications in wave propagation", *J. Mech. Phys. Solids*, **78**, 298-313. https://doi.org/10.1016/j.jmps.2015.02.001

Lu, L., Guo, X. and Zhao, J. (2017), "Size-dependent vibration analysis of nanobeams based on the nonlocal strain gradient theory", *Int. J. Eng. Sci.*, **116**, 12-24. https://doi.org/10.1016/j.ijengsci.2017.03.006

Ma, L.H., Ke, L.L., Reddy, J.N., Yang, J., Kitipornchai, S. and Wang, Y.S. (2018), "Wave propagation characteristics in magneto-electro-elastic nanoshells using nonlocal strain gradient theory", *Compos. Struct.*, **199**, 10-23. https://doi.org/10.1016/j.compstruct.2018.05.061

Mehralian, F., Beni, Y.T. and Zeverdejani, M.K. (2017), "Calibration of nonlocal strain gradient shell model for buckling analysis of nanotubes using molecular dynamics simulations", *Physica B*: *Condensed Matter*, **521**, 102-111. https://doi.org/10.1016/j.physb.2017.06.058

Pan, E. (2001), "Exact solution for simply supported and multilayered magneto-electro-elastic plates", *J. Appl. Mech.*, **68**(4), 608-618. https://doi.org/10.1115/1.1380385

Park, W.T., Han, S.C., Jung, W.Y. and Lee, W.H. (2016), "Dynamic instability analysis for S-FGM plates embedded in Pasternak elastic medium using the modified couple stress theory", *Steel Compos. Struct., Int. J.*, **22**(6), 1239-1259. https://doi.org/10.12989/scs.2016.22.6.1239

Ramirez, F., Heyliger, P.R. and Pan, E. (2006), "Free vibration response of two-dimensional magneto-electro-elastic laminated plates", *J. Sound Vib.*, **292**(3-5), 626-644. https://doi.org/10.1016/j.jsv.2005.08.004

She, G.L., Yuan, F.G., Ren, Y.R., Liu, H.B. and Xiao, W.S. (2018), "Nonlinear bending and vibration analysis of functionally graded porous tubes via a nonlocal strain gradient theory", *Compos. Struct.*, **203**, 614-623. https://doi.org/10.1016/j.compstruct.2018.07.063

Şimşek, M. (2019), "Some closed-form solutions for static, buckling, free and forced vibration of functionally graded (FG) nanobeams using nonlocal strain gradient theory", *Compos. Struct.*, **224**, 111041. https://doi.org/10.1016/j.compstruct.2019.111041

Waksmanski, N. and Pan, E. (2017), "An analytical three-dimensional solution for free vibration of a magneto-electro-elastic plate considering the nonlocal effect", *J. Intel. Mater. Syst. Struct.*, **28**(11), 1501-1513. https://doi.org/10.1177%2F1045389X16672734

Zeighampour, H., Beni, Y.T. and Dehkordi, M.B. (2018), "Wave propagation in viscoelastic thin cylindrical nanoshell resting on a visco-Pasternak foundation based on nonlocal strain gradient theory", *Thin-Wall. Struct.*, **122**, 378-386. https://doi.org/10.1016/j.tws.2017.10.037

CC

Appendix

$$n_1 = \int_0^L \int_0^{2\pi R} ((1-l^2\nabla^2)\left[A_{11}\left(\frac{\partial^2 \bar{w}}{\partial x^2}\frac{\partial \bar{w}}{\partial x}\right) + A_{12}\left(\frac{\partial^2 \bar{w}}{\partial x \partial y}\frac{\partial \bar{w}}{\partial y}\right) + A_{66}\left(+\frac{\partial^2 \bar{w}}{\partial x \partial y}\frac{\partial \bar{w}}{\partial y} + \frac{\partial \bar{w}}{\partial x}\frac{\partial^2 \bar{w}}{\partial y^2}\right)\right]\right)\bar{u}(x,y)dydx \tag{A1}$$

$$n_2 = \int_0^L \int_0^{2\pi R} ((1-l^2\nabla^2)\left[A_{66}\left(\frac{\partial^2 w}{\partial x^2}\frac{\partial w}{\partial y} + \frac{\partial w}{\partial x}\frac{\partial^2 w}{\partial x \partial y}\right) + A_{12}\left(\frac{\partial w}{\partial x}\frac{\partial^2 w}{\partial x \partial y}\right) + A_{11}\left(\frac{\partial^2 w}{\partial y^2}\frac{\partial w}{\partial y}\right)\right]\right)\bar{v}(x,y)dydx \tag{A2}$$

$$\begin{aligned} n_3 = \int_0^L \int_0^{2\pi R} \Bigg(& (1-l^2\nabla^2)\left[B_{11}\left(\frac{\partial^3 u}{\partial x^3} + \frac{\partial^3 w}{\partial x^3}\frac{\partial w}{\partial x} + \frac{\partial^2 w}{\partial x^2}\frac{\partial^2 w}{\partial x^2}\right) + B_{12}\left(\frac{\partial^3 w}{\partial x^2 \partial y}\frac{\partial w}{\partial y} + \frac{\partial^2 w}{\partial x \partial y}\frac{\partial^2 w}{\partial x \partial y}\right)\right. \\ & +2B_{66}\left(\frac{\partial^2 w}{\partial x^2}\frac{\partial^2 w}{\partial y^2} + \frac{\partial w}{\partial x}\frac{\partial^3 w}{\partial x \partial y^2} + \frac{\partial^3 w}{\partial x^2 \partial y}\frac{\partial w}{\partial y} + \frac{\partial^2 w}{\partial x \partial y}\frac{\partial^2 w}{\partial x \partial y}\right) \\ & +B_{12}\left(\frac{\partial w}{\partial x}\frac{\partial^3 w}{\partial x \partial y^2} + \frac{\partial^2 w}{\partial x \partial y}\frac{\partial^2 w}{\partial x \partial y}\right) + B_{11}\left(\frac{\partial^3 w}{\partial y^3}\frac{\partial w}{\partial y} + \frac{\partial^2 w}{\partial y^2}\frac{\partial^2 w}{\partial y^2}\right) + \frac{A_{12}}{R}\left(\frac{1}{2}\left(\frac{\partial w}{\partial x}\right)^2\right) \\ & \left. + \frac{A_{11}}{R}\left(\frac{1}{2}\left(\frac{\partial w}{\partial y}\right)^2\right)\right] + (1-(ea)^2\nabla^2)((1-l^2\nabla^2) \\ & -B_{11}\frac{\partial^2 w}{\partial x^2} + A_{12}\left(-\frac{w}{R}\right) - B_{12}\left(\frac{\partial^2 w}{\partial y^2}\right)\Bigg)\left(\frac{\partial^2 w}{\partial x^2}\right) \\ & +2(1-(ea)^2\nabla^2)((1-l^2\nabla^2) \\ & \left[-2B_{66}\frac{\partial^2 w}{\partial x \partial y}\right]\Bigg)\left(\frac{\partial^2 w}{\partial x \partial y}\right) \\ & +(1-(ea)^2\nabla^2)((1-l^2\nabla^2)\left[-B_{12}\frac{\partial^2 w}{\partial x^2}\right. \\ & \left. +A_{11}\left(-\frac{w}{R}\right) - B_{11}\frac{\partial^2 w}{\partial y^2}\right]\Bigg)\left(\frac{\partial^2 w}{\partial y^2}\right)\Bigg)\bar{w}(x,y)dydx \end{aligned} \tag{A3}$$

$$\begin{aligned} n_4 = \int_0^L \int_0^{2\pi R} & (+ (1-(ea)^2\nabla^2)((1-l^2\nabla^2) \\ & \left[A_{11}\left(\frac{1}{2}\left(\frac{\partial w}{\partial x}\right)^2\right) + A_{12}\left(\frac{1}{2}\left(\frac{\partial w}{\partial y}\right)^2\right)\right]\Bigg)\left(\frac{\partial^2 w}{\partial x^2}\right) \\ & +2(1-(ea)^2\nabla^2)((1-l^2\nabla^2) \\ & \left[A_{66}\left(\frac{\partial w}{\partial x}\frac{\partial w}{\partial y}\right)\right]\Bigg)\left(\frac{\partial^2 w}{\partial x \partial y}\right) \\ & +(1-(ea)^2\nabla^2)((1-l^2\nabla^2)\left[A_{12}\left(\frac{1}{2}\left(\frac{\partial w}{\partial x}\right)^2\right)\right. \\ & \left. +A_{11}\left(\frac{1}{2}\left(\frac{\partial w}{\partial y}\right)^2\right)\right]\Bigg)\left(\frac{\partial^2 w}{\partial y^2}\right)\Bigg)\bar{w}(x,y)dydx \end{aligned} \tag{A4}$$

$$n_5 = \int_0^L \int_0^{2\pi R} ((1-(ea)^2\nabla^2)((1-l^2\nabla^2) \tag{A5}$$

$$\left[A_{11}\left(\frac{\partial u}{\partial x}\right)\right]\left)\left(\frac{\partial^2 w}{\partial x^2}\right)+2(1-(ea)^2\nabla^2)\right.$$
$$\left((1-l^2\nabla^2)\left[A_{66}\left(\frac{\partial u}{\partial y}\right)\right]\right)\left(\frac{\partial^2 w}{\partial x\partial y}\right)$$
$$+(1-(ea)^2\nabla^2)((1-l^2\nabla^2)\left[A_{12}\left(\frac{\partial u}{\partial x}\right)\right]\right)$$
$$\left.\left(\frac{\partial^2 w}{\partial y^2}\right)\right)\bar{w}(x,y)dydx \tag{A5}$$

$$n_6=\int_0^L\int_0^{2\pi}(\,(1-(ea)^2\nabla^2)((1-l^2\nabla^2)$$
$$\left[+A_{12}\left(\frac{\partial v}{\partial y}\right)\right]\left)\left(\frac{\partial^2 w}{\partial x^2}\right)+2(1-(ea)^2\nabla^2)\right.$$
$$\left((1-l^2\nabla^2)\left[A_{66}\left(\frac{\partial v}{\partial x}\right)\right]\right)\left(\frac{\partial^2 w}{\partial x\partial y}\right) \tag{A6}$$
$$+(1-(ea)^2\nabla^2)((1-l^2\nabla^2)\left[+A_{11}\left(\frac{\partial v}{\partial y}\right)\right]\right)$$
$$\left.\left(\frac{\partial^2 w}{\partial y^2}\right)\right)\bar{w}(x,y)dydx$$

$$n_7=\int_0^L\int_0^{2\pi R}\left(+A_{31}^e\left(\frac{1}{2}\left(\frac{\partial w}{\partial x}\right)^2+\frac{1}{2}\left(\frac{\partial w}{\partial y}\right)^2\right)\right)\bar{\phi}(x,y)dydx \tag{A7}$$

$$n_8=\int_0^L\int_0^{2\pi R}\left(+A_{31}^m\left(\frac{1}{2}\left(\frac{\partial w}{\partial x}\right)^2+\frac{1}{2}\left(\frac{\partial w}{\partial y}\right)^2\right)\right)\bar{\gamma}(x,y)dydx \tag{A8}$$

$$n_9=\int_0^L\int_0^{2\pi R}\left(+(1-(ea)^2\nabla^2)(+A_{31}^e\phi)\left(\frac{\partial^2 w}{\partial x^2}\right)\right.$$
$$\left.+(1-(ea)^2\nabla^2)(+A_{31}^e\phi)\left(\frac{\partial^2 w}{\partial y^2}\right)\right)\bar{w}(x,y)dydx \tag{A9}$$

$$n_{10}=\int_0^L\int_0^{2\pi R}\left(+(1-(ea)^2\nabla^2)(A_{31}^m\gamma)\left(\frac{\partial^2 w}{\partial x^2}\right)\right.$$
$$\left.+(1-(ea)^2\nabla^2)(A_{31}^m\gamma)\left(\frac{\partial^2 w}{\partial y^2}\right)\right)\bar{w}(x,y)dydx \tag{A10}$$

and

$$k_{11}=\int_0^L\int_0^{2\pi R}\left((1-l^2\nabla^2)\left[A_{11}\frac{\partial^2\bar{u}}{\partial x^2}+A_{66}\left(\frac{\partial^2\bar{u}}{\partial y^2}\right)\right]\right)\bar{u}(x,y)dydx \tag{A11}$$

$$k_{21}=\int_0^L\int_0^{2\pi R}\left((1-l^2\nabla^2)\left[A_{12}\left(\frac{\partial^2\bar{v}}{\partial x\partial y}\right)+A_{66}\left(\frac{\partial^2\bar{v}}{\partial x\partial y}\right)\right]\right)\bar{u}(x,y)dydx \tag{A12}$$

$$k_{31}=\int_0^L\int_0^{2\pi R}\left((1-l^2\nabla^2)\left[-B_{11}\frac{\partial^3 w}{\partial x^3}+A_{12}\left(-\frac{1}{R}\frac{\partial w}{\partial x}\right)-B_{12}\frac{\partial^3 w}{\partial x\partial y^2}-2B_{66}\frac{\partial^3 w}{\partial x\partial y^2}\right]\right)u(x,y)dydx \tag{A13}$$

$$k_{41}=\int_0^L\int_0^{2\pi R}\left(A_{31}^e\frac{\partial\phi}{\partial x}\right)u(x,y)dydx \tag{A14}$$

$$k_{51}=\int_0^L\int_0^{2\pi R}\left(A_{31}^m\frac{\partial\gamma}{\partial x}\right)u(x,y)dydx \tag{A15}$$

$$k_{12}=\int_0^L\int_0^{2\pi R}\left((1-l^2\nabla^2)\left[A_{66}\left(\frac{\partial^2 u}{\partial x\partial y}\right)+A_{12}\frac{\partial^2 u}{\partial x\partial y}\right]\right)v(x,y)dydx \tag{A16}$$

$$k_{22}=\int_0^L\int_0^{2\pi R}\left((1-l^2\nabla^2)\left[A_{66}\left(\frac{\partial^2 v}{\partial x^2}\right)+A_{11}\left(\frac{\partial^2 v}{\partial y^2}\right)\right]\right)v(x,y)dydx \tag{A17}$$

$$k_{32}=\int_0^L\int_0^{2\pi R}\left((1-l^2\nabla^2)\left[-2B_{66}\frac{\partial^3 w}{\partial x^2\partial y}z-B_{12}\frac{\partial^3 w}{\partial x^2\partial y}+A_{11}\left(-\frac{1}{R}\frac{\partial w}{\partial y}\right)-B_{11}\frac{\partial^3 w}{\partial y^3}\right]\right)v(x,y)dydx \tag{A18}$$

$$k_{42}=\int_0^L\int_0^{2\pi R}\left(+A_{31}^e\frac{\partial\phi}{\partial y}\right)v(x,y)dydx \tag{A19}$$

$$k_{52}=\int_0^L\int_0^{2\pi R}\left(+A_{31}^m\frac{\partial\gamma}{\partial y}\right)v(x,y)dydx \tag{A20}$$

$$k_{13}=\int_0^L\int_0^{2\pi R}\left((1-l^2\nabla^2)\left[B_{11}\frac{\partial^3 u}{\partial x^3}+2B_{66}\left(\frac{\partial^3 u}{\partial x\partial y^2}\right)+B_{12}\frac{\partial^3 u}{\partial x\partial y^2}+\frac{A_{12}}{R}\frac{\partial u}{\partial x}\right]\right)w(x,y)dydx \tag{A21}$$

$$k_{23}=\int_0^L\int_0^{2\pi R}\left((1-l^2\nabla^2)\left[+B_{12}\left(\frac{\partial^3 v}{\partial x^2\partial y}\right)+2B_{66}\left(\frac{\partial^3 v}{\partial x^2\partial y}\right)+B_{11}\left(\frac{\partial^3 v}{\partial y^3}\right)+\frac{A_{11}}{R}\left(\frac{\partial v}{\partial y}\right)\right]\right)w(x,y)dydx \tag{A22}$$

$$k_{33}=\int_0^L\int_0^{2\pi R}\left((1-l^2\nabla^2)\left[-D_{11}\frac{\partial^4 w}{\partial x^4}\right.\right. \tag{A23}$$

$$+B_{12}\left(-\frac{1}{R}\frac{\partial^2 w}{\partial x^2}\right)-2D_{12}\frac{\partial^4 w}{\partial x^2\partial y^2}$$
$$-4D_{66}\frac{\partial^4 w}{\partial x^2\partial y^2}+B_{11}\left(-\frac{1}{R}\frac{\partial^2 w}{\partial y^2}\right)-D_{11}\frac{\partial^4 w}{\partial y^4}$$
$$-\frac{B_{12}}{R}\frac{\partial^2 w}{\partial x^2}+\frac{A_{11}}{R}\left(-\frac{w}{R}\right)-\frac{B_{11}}{R}\frac{\partial^2 w}{\partial y^2}\Bigg] \quad \text{(A23)}$$
$$+(1-(ea)^2\nabla^2)[-(N^E+N^H+N^M)$$
$$\left(\frac{\partial^2 w}{\partial x^2}+\frac{\partial^2 w}{\partial y^2}\right)\Bigg]\Bigg)w(x,y)dydx$$

$$k_{43}=\int_0^L\int_0^{2\pi R}\left(+E_{31}^e\left(\frac{\partial^2\phi}{\partial x^2}+\frac{\partial^2\phi}{\partial y^2}\right)+\frac{A_{31}^e}{R}\phi\right)w(x,y)dydx \quad \text{(A24)}$$

$$k_{53}=\int_0^L\int_0^{2\pi R}\left(+E_{31}^m\left(\frac{\partial^2\gamma}{\partial x^2}+\frac{\partial^2\gamma}{\partial y^2}\right)+\frac{A_{31}^m}{R}\gamma\right)w(x,y)dydx \quad \text{(A25)}$$

$$k_{14}=\int_0^L\int_0^{2\pi R}\left(+A_{31}^e\left(\frac{\partial u}{\partial x}\right)\right)\phi(x,y)dydx \quad \text{(A26)}$$

$$k_{24}=\int_0^L\int_0^{2\pi R}\left(+A_{31}^e\left(+\frac{\partial v}{\partial y}\right)\right)\phi(x,y)dydx \quad \text{(A27)}$$

$$k_{34}=\int_0^L\int_0^{2\pi R}\left(+A_{31}^e\left(-\frac{w}{R}\right)-E_{31}^e\left(\frac{\partial^2 w}{\partial x^2}+\frac{\partial^2 w}{\partial y^2}\right)\right)\phi(x,y)dydx \quad \text{(A28)}$$

$$k_{44}=\int_0^L\int_0^{2\pi R}\left(+F_{11}^e\frac{\partial^2\phi}{\partial x^2}+F_{22}^e\frac{\partial^2\phi}{\partial y^2}-F_{33}^e\phi\right)\phi(x,y)dydx \quad \text{(A29)}$$

$$k_{54}=\int_0^L\int_0^{2\pi R}\left(+F_{11}^m\frac{\partial^2\gamma}{\partial x^2}+F_{22}^m\frac{\partial^2\gamma}{\partial y^2}-F_{33}^m\gamma\right)\phi(x,y)dydx \quad \text{(A30)}$$

$$k_{15}=\int_0^L\int_0^{2\pi R}\left(+A_{31}^m\left(\frac{\partial u}{\partial x}\right)\right)\gamma(x,y)dydx \quad \text{(A31)}$$

$$k_{25}=\int_0^L\int_0^{2\pi R}\left(+A_{31}^m\left(+\frac{\partial v}{\partial y}\right)\right)\gamma(x,y)dydx \quad \text{(A32)}$$

$$k_{35}=\int_0^L\int_0^{2\pi R}\left(+A_{31}^m\left(-\frac{w}{R}\right)-E_{31}^m\left(\frac{\partial^2 w}{\partial x^2}+\frac{\partial^2 w}{\partial y^2}\right)\right)\gamma(x,y)dydx \quad \text{(A33)}$$

$$k_{55}=\int_0^L\int_0^{2\pi R}\left(+X_{11}^m\frac{\partial^2\bar{\gamma}}{\partial x^2}+X_{22}^m\frac{\partial^2\bar{\gamma}}{\partial y^2}-X_{33}^m\bar{\gamma}\right)\bar{\gamma}(x,y)dydx \quad \text{(A34)}$$